December 2006

Identification of a Putative Operon Involved in Fructooligosaccharide Utilization by *Lactobacillus paracasei*

Yong Jun Goh
University of Nebraska-Lincoln

Andrew K. Benson
University of Nebraska-Lincoln, abenson1@unl.edu

Vicki Schlegel
University of Nebraska-Lincoln, vschlegel3@unl.edu

Jong-Hwa Lee
University of Nebraska-Lincoln

Robert W. Hutkins
University of Nebraska-Lincoln, rhutkins1@unl.edu

APPLIED AND ENVIRONMENTAL MICROBIOLOGY, Dec. 2006, p. 7518–7530 Vol. 72, No. 12
0099-2240/06/$08.00+0 doi:10.1128/AEM.00877-06

Identification of a Putative Operon Involved in Fructooligosaccharide Utilization by *Lactobacillus paracasei*▽†

Yong Jun Goh,§ Chaomei Zhang, Andrew K. Benson, Vicki Schlegel, Jong-Hwa Lee,¶ and Robert W. Hutkins*

Department of Food Science and Technology, University of Nebraska, Lincoln, Nebraska 68583-0919

Received 13 April 2006/Accepted 25 September 2006

The growth and activity of some *Lactobacillus* and *Bifidobacterium* strains are stimulated by the presence of nondigestible fructooligosaccharides (FOS), which are selectively fermented by specific intestinal bacteria. Consumption of FOS, therefore, enriches for those bacteria that possess metabolic pathways necessary for FOS metabolism. In this study, a DNA microarray consisting of 7,680 random genomic library fragments of *Lactobacillus paracasei* 1195 was used to examine genes involved in the utilization of FOS in this organism. Differential expression profiles between cells grown on FOS and those grown on glucose provided a basis for identifying genes specifically induced by FOS. Several of the FOS-induced genes shared sequence identity with genes encoding β-fructosidases and components of phosphoenolpyruvate-dependent phosphotransferase systems (PTS). These genes were organized in a putative operon, designated the *fos* operon, that may play an essential role in FOS utilization. The complete 7,631-bp nucleotide sequence of the putative *fos* operon was determined and consists of *fosABCDXE* genes, which encode a putative fructose/mannose PTS (FosABCDX) and a β-fructosidase precursor (FosE). The latter contains an N-terminal signal peptide sequence and cell wall sorting signals at the C-terminal region, suggesting its localization at the cell wall. Inactivation of the *fosE* gene led to impaired growth on FOS and other β-fructose-linked carbohydrates. Transcriptional analysis by reverse transcriptase PCR suggested that *fosABCDXE* was cotranscribed as a single mRNA during growth on FOS. Expression array analysis revealed that when glucose was added to FOS-grown cells, transcription of the FOS-induced genes was repressed, indicating that FOS metabolism is subject to catabolite regulation.

Probiotic bacteria have attracted much commercial and research interest due to their role in promoting human intestinal health. These bacteria, usually species of *Bifidobacterium* and *Lactobacillus*, confer various beneficial effects on the host, especially by reducing the incidence of intestinal diseases (14, 21, 47). It has also been suggested that the colonic population of autochthonous or exogenous probiotic bacteria is significantly influenced by those nondigestible oligosaccharides that reach the colon (12). These so-called prebiotic carbohydrates are selectively metabolized by a limited number of microorganisms residing in the colon, including *Bifidobacterium* and *Lactobacillus*. In particular, independent studies (11, 13, 16, 52) have shown that the growth and activity of these bacteria are stimulated by fructooligosaccharides (FOS), prebiotic fructans that are either derived from inulin and other edible plant materials or synthesized enzymatically from sucrose via transfructosylation (17, 18, 37). Among the commercial FOS products are linear fructose oligomers consisting of a glucose monomer (G) linked α-1,2 to two or more β-2,1-linked fructosyl units (F), forming a mixture of 1-kestose (GF_2), nystose (GF_3), and 1^F-fructofuranosyl nystose (GF_4), referred to collectively as GF_n-type FOS (38). Another type of FOS, commonly known as oligofructose, or FF_n-type FOS, is produced by the partial hydrolysis of chicory inulin using an endoinulinase and is characterized by a degree of polymerization varying from 2 to 10, with an average degree of polymerization of 4 (37). The ability to utilize FOS may provide selective advantages to probiotic bacteria in the intestinal tract, resulting in the suppression or displacement of undesirable or pathogenic bacteria (2, 6, 36).

Although the prebiotic effects of FOS on enteric populations have been demonstrated both in vivo and in vitro, the molecular mechanisms by which FOS metabolism occurs in *Bifidobacterium* and *Lactobacillus* have only recently been investigated. In bifidobacteria, cytoplasmic β-fructosidases that catalyze the hydrolysis of FOS in *Bifidobacterium adolescentis*, *Bifidobacterium infantis*, and *Bifidobacterium lactis* have been isolated and characterized (19, 20, 31–33, 40, 50). More recently, the gene encoding β-fructofuranosidase in *B. lactis* $DSM10140^T$ has been cloned and expressed in *Escherichia coli* (10, 20). In addition, the genome sequence of *Bifidobacterium longum* revealed the presence of at least seven regions coding for oligosaccharide transport and metabolism (48). The authors of that study suggested that the function of these oligosaccharide-metabolizing pathways is to provide bifidobacteria with the ability to compete and persist in the colon, where nondigestible oligosaccharides are likely to accumulate.

Based on an in silico analysis of the *Lactobacillus acidophilus* NCFM genome sequence, Barrangou et al. (3) previously identified a gene cluster encoding an oligofructose metabolic path-

* Corresponding author. Mailing address: Department of Food Science and Technology, University of Nebraska, 338 FIC, Lincoln, NE 68583-0919. Phone: (402) 472-2820. Fax: (402) 472-1693. E-mail: rhutkins1@unl.edu.

† Supplemental material for this article may be found at http://aem.asm.org/.

§ Present address: Department of Food Science, North Carolina State University, Raleigh, NC 27695-7624.

¶ Present address: School of Bioresource Sciences, Andong National University, Andong, South Korea.

▽ Published ahead of print on 6 October 2006.

way. Functional analysis of this gene cluster indicated that the uptake of oligofructose was mediated by an ATP-dependent binding cassette (ABC)-type transport system. Genes encoding the ABC transport system (*msmEFGK*) as well as a putative intracellular fructosidase (*bfrA*) are located in a multiple-sugar metabolism (*msm*) operon. All of the genes in this operon were coexpressed in the presence of sucrose and both GF_n- and FF_n-type FOS but not glucose or fructose. The genetic organization of this operon exhibits a high degree of synteny with the *msm* operon in *Streptococcus mutans* and the raffinose (*raf*) operon in *Streptococcus pneumoniae* (43, 45). Similarly, Kaplan and Hutkins (22) previously provided biochemical evidence to suggest that the uptake of FOS by *Lactobacillus paracasei* 1195 was also mediated by an ABC transport system. This system showed a preference for GF_2 and GF_3, whereas little GF_4 was apparently transported. In addition, the transport system appeared to be specific for FOS and possibly other substrates with a β-fructose or β-type sugar linked to α-glucose. FOS hydrolysis activity was detected only in the cell extracts of FOS- or sucrose-grown cells and was absent in cell-free culture supernatants, indicating that FOS hydrolysis was mediated by an intracellular β-fructofuranosidase. Both FOS transport and hydrolysis activities were induced by growth on sucrose and FOS and repressed by products of their hydrolysis, glucose and fructose.

Here, we describe a shotgun microarray-based approach to identify the genes encoding the FOS utilization pathway in *L. paracasei* 1195. Our results revealed the presence of an operon that encodes a cell surface-anchored fructosidase and a fructose phosphotransferase system (PTS) that are likely involved in the hydrolysis of FOS and the subsequent transport of free fructose into the cytoplasm, respectively.

MATERIALS AND METHODS

Organisms and growth conditions. *Lactobacillus paracasei* 1195, from the University of Nebraska Department of Food Science and Technology Culture Collection, was routinely propagated in MRS broth (Difco, Inc., Ann Arbor, MI) statically at 37°C in ambient atmosphere. For gene expression analyses, cells were grown in modified MRS (mMRS) basal medium containing (per liter): 5 g proteose peptone no. 3 (Difco), 5 g beef extract (Difco), 2.5 g yeast extract (Difco), 1 g polysorbate 80 (Fisher Chemicals, Fairlawn, NJ), 2 g ammonium citrate (Sigma-Aldrich, St. Louis, MO), 5 g sodium acetate (Sigma), 0.1 g magnesium sulfate (Sigma), 0.05 g manganese sulfate (Sigma), and 2 g dipotassium phosphate (MCB Manufacturing Chemists, Norwood, OH). Filter-sterilized solutions of FOS (GTC Nutrition, Westminster, CO) or glucose (Sigma) were added to a final concentration of 1 to 2% (wt/vol) where indicated.

Escherichia coli strains One Shot TOP10 (Invitrogen Life Technologies, Carlsbad, CA), DH5α (Gibco, Rockville, MD), and EC1000 (25) were grown in Luria-Bertani (LB) medium at 37°C with aeration at 200 rpm. When necessary, kanamycin (Kan) (Sigma), ampicillin (Sigma), or erythromycin (Erm) (Sigma) was added at concentrations of 40 to 50 μg/ml, 100 μg/ml, and 450 μg/ml, respectively. Recombinant *L. paracasei* strains were selected and maintained on 2 to 5 μg/ml of Erm and/or chloramphenicol (Sigma) where indicated.

DNA isolation and manipulations. For the isolation of genomic DNA from *L. paracasei* 1195, two milliliters of a culture grown overnight was inoculated into 100 ml of fresh MRS broth. The cells were grown to an optical density at 625 nm (OD_{625}) of ≈0.6, collected by centrifugation, washed with 20 ml of STE buffer (50 mM NaCl, 100 mM Tris, 70 mM EDTA, pH 8.0), and resuspended in 12.5 ml of fresh STE buffer. Lysis of cells was achieved by adding 100 mg of lysozyme (Sigma), 200 μl of 10× Bactozyme (Molecular Research Center, Inc., Cincinnati, OH), and 1,000 U of mutanolysin (Sigma), followed by incubation at 37°C overnight. The cell lysate was treated with sodium dodecyl sulfate (1% final concentration) and 6 mg of proteinase K (Sigma) at 55 to 60°C for 2 to 3 h. Chromosomal DNA was sequentially extracted with phenol and chloroform-isoamyl alcohol (24:1), precipitated with ethanol, washed, and dissolved in Tris-EDTA buffer. Routine plasmid DNA isolation from *E. coli* was performed by using a standard alkaline lysis method (5). For DNA sequencing, plasmid DNA was purified from *E. coli* using a QIAprep Spin Miniprep kit (QIAGEN Inc., Valencia, CA) or a Zyppy Plasmid Miniprep I kit (Zymo Research Corp., Orange, CA) according to the manufacturer's instructions.

Primers used in this study (Table 1) were synthesized by Sigma-Genosys (The Woodlands, TX). PCR amplifications were performed by using an Amplitron II Thermolyne thermocycler (Barnstead/Thermolyne Corp., Dubuque, IA). DNA fragments from agarose gels were purified using a QIAquick gel extraction kit (QIAGEN) or a Zymoclean Gel DNA recovery kit (Zymo Research). DNA sequencing was performed by the Genome Core Research Facility (University of Nebraska—Lincoln) and the Genomics Technology Support Facility (Michigan State University, East Lansing, Mich.).

E. coli DH5α and EC1000 competent cells were prepared and transformed according to procedures described previously by Hanahan (15). Preparation of *L. paracasei* cells for electrotransformation was performed according to a protocol optimized as described previously by Wei et al. (51), with the following modifications: during washing steps, cells (from a 100-ml culture) were washed with 10 ml and 50 ml of ice-cold washing buffer (272 mM sucrose, 1 mM $MgCl_2$, 7 mM potassium phosphate buffer, pH 7.4) sequentially, followed by a third wash with 10 ml of ice-cold 10% glycerol, and finally resuspended in 1/100 of the initial culture volume with ice-cold 10% glycerol.

Construction of genomic library and preparation of DNA microarrays. Genomic DNA was mechanically sheared and size fractionated on a 0.8% (wt/vol) agarose gel. Fragments of 1 to 4 kb were purified from gels and ligated into the pCR-Blunt II-TOPO vector using a Zero Blunt TOPO cloning kit (Invitrogen) based on the manufacturer's instructions. The ligation products were subsequently electroporated into One Shot TOP10 Electrocomp *E. coli* cells at 12.5 kV cm^{-1}, 200 Ω, and 25 μF using a Gene Pulser electroporation system (Bio-Rad Laboratories, Inc., Hercules, CA). A total of 7,680 independent clones were selected and grown in individual wells of 96-well round-bottom microtiter plates (Corning Corp., Corning, NY) containing 120 μl of LB supplemented with Kan. For amplification of the cloned genomic fragments, 2 μl of each cell suspension was used as an amplification template in 50-μl PCR mixtures containing 200 μM of each deoxynucleotide triphosphate (dNTP) (Takara Mirus Bio Inc., Madison, WI), 2.4 mM $MgCl_2$, 50 pmol each M13-for and M13-rev primers (Table 1), and 2.5 U of *Taq* DNA polymerase in 1× PCR buffer (Sigma). PCR amplifications were performed in 96-well PCR plates, and aliquots of the PCR products were analyzed on agarose gels (with an average size of 1.5 kb). The remaining amplified mixtures were transferred into 96-well microtiter plates, precipitated by the addition of 0.1 volume of 3 M sodium acetate (pH 5.2) and 2 volumes of ice-cold ethanol, washed, and resuspended in 30 μl of 3× SSC (1× SSC is 0.15 M NaCl plus 0.015 M sodium citrate). The purified amplicons were spotted onto silanated glass slides (CEL Associates, Inc., Pearland, TX) in four subarrays (2 × 2 format); each subarray consisted of 44 × 44 clones using an OmniGrid robotic arrayer (GeneMachine, San Carlos, CA). Pretreatment of microarrays for hybridization was performed as described in the Sigma technical bulletin for the ArrayHyb LowTemp hybridization buffer (http://www.sigmaaldrich.com/sigma/bulletin/a3095bul.pdf).

Experimental design and RNA purification. For sugar induction experiments (FOS versus glucose), *L. paracasei* cells (2% [vol/vol] inoculum from a culture grown overnight in MRS broth) were grown in 300 ml of mMRS basal medium (with no added sugar source), and the cell density was monitored using a spectrophotometer (Beckman DU-640; Beckman Coulter, Inc., Fullerton, CA). When the culture reached a final OD_{625} of ≈0.3, at which point all of the residual sugars in the medium were consumed (based on high-performance liquid chromatography [HPLC] analysis of the supernatants), the culture was then divided into two 150-ml portions, where FOS or glucose was added to a 1% final concentration. Cells were collected for total RNA isolation after 30 min (OD_{625} ≈ 0.3 to 0.4). For the glucose repression experiment (FOS versus FOS plus glucose), cells (2% inoculum from a culture grown overnight in MRS broth) were grown in 100 ml of mMRS medium supplemented with 2% FOS until an OD_{625} of ≈0.6 was reached. The culture was split into two 50-ml portions, and glucose was added to one of the portions at a 2% final concentration. Both cultures were grown for another 60 min (OD_{625} ≈ 1.0) before being harvested for total RNA isolation. Both experiments were performed in independent replicates (two biological replicates per experiment) with incubation at 37°C in an ambient atmosphere. For total RNA extraction, cells were collected by centrifugation at 9,820 × *g* for 8 min at room temperature. Cell pellets were resuspended in 1 ml of TRI reagent (Molecular Research Center) and transferred into 1.5-ml conical tubes (BioSpec Products, Inc., Bartlesville, OK) containing ≈400 mg of 0.1-mm-diameter glass beads (BioSpec Products). The mixture was homogenized with a Mini-Beadbeater (BioSpec Products) at 4,200 rpm for six

TABLE 1. Primers used in this study

Primer[a]	Sequence (5′–3′)	Application
Construction of shotgun microarray		
M13-for	GTAAAACGACGGCCAG	Amplification of shotgun library fragments
M13-rev	CAGGAAACAGCTATGAC	
RT-PCR analysis		
LP1195-16Sfor	TGGAGAGTTTGATCCTGGCTC	Semiquantitative analysis of 16S rRNA transcript level
LP1195-16Srev	GCTGCTGGCACGTAGTTAGC	
lpca3-04E05for	GGTTTCTAAACGCTTCTGCTCG	Semiquantitative analysis of array clone 04E05 transcript level encoding putative fructose PTS components IIC and IID
lpca3-04E05rev	CGACATACCAAGGGAAATCC	
lpca1-62G02for	TGGAAATGGATGAAAAGAAA	Semiquantitative analysis of array clone 62G02 transcript level encoding N-terminal region of a β-fructosidase
lpca1-62G02rev	TGTTAACCGCATCGTAGACC	
lpca1-15A08for	GGACTGGACATATGCTTCTA	Semiquantitative analysis of array clone 15A08 transcript level encoding central region of a β-fructosidase
lpca1-15A08rev	ACCGTAATTGTAATTGATCC	
FosA7	GTCCACTCACAACGGTTTGC	Confirm cotranscription of putative *fos* operon
FosD2	CGACATACCAAGGGAAATCC	
FosD44	ATGATGACCAGGTCAAAGCC	Confirm cotranscription of putative *fos* operon
FosE24	TGTTAACCGCATCGTAGACC	
Contig gap closure		
lpca2-lpca3for	GTCCACTCACAACGGTTTGC	Determine DNA sequence of lpca2–lpca3 gap region
lpca2-lpca3rev	CGAGCAGAAGCGTTTAGAAACC	
lpca3-lpca1for	AGCGGCAACCAGAAGATTTC	Determine DNA sequence of lpca3–lpca1 gap region
lpca3-lpca1rev	TGGTTGCAATTGTTGCGGAC	
Genome walking upstream of contig lpca2		
lpca2UP_1for	CAATCGTCTATCCAACACATGG	Determine upstream flanking sequence of lpca2, first-round tailed PCR
lpca2UP_1nes	GGGACACTCAAAAAGAAGTTGC	
lpca2UP_2for	CTTGCCAGACACACAATCAGC	Second-round tailed PCR
lpca2UP_2nes	TACAATGCCATCCTGCTTGCTC	
lpca2UP_3for	CCAGCACTTGAAGTCATTGC	Third-round tailed PCR
lpca2UP_3nes	TCCATACCCTGCTCACCAATC	
Poly(G)	ATATGGGGGAGGGGGAGGGGG	Used with nested primers to amplify tailed fragments

[a] for, forward; rev, reverse; nes, nested.

1-min cycles. The samples were cooled on ice for 1 min between each cycle. All subsequent RNA isolation procedures were performed according to instructions supplied with the TRI reagent. RNA samples were subsequently treated with DNase I using a DNA*free* kit (Ambion Inc., Austin, TX), purified through RNeasy Mini kit columns (QIAGEN), and concentrated using Amicon Microcon YM-30 columns (Millipore Corp., Billerica, MA) to a final concentration of ≥3 μg/ml. The quality and integrity of the purified RNA samples were monitored using a spectrophotometer (A_{260}/A_{280} ratio of 1.6 to 1.9) and by electrophoresis in a 1% (wt/vol) agarose gel in standard 1× Tris-borate-EDTA buffer. Denaturation treatment of RNA samples prior to gel electrophoresis was performed by mixing 2 μl of each RNA sample (5 to 10 μg) with 18 μl of formamide followed by incubation at 65°C for 10 min. The absence of contaminating DNA was verified by PCR amplification with 5 μg of purified RNA sample as a template with the primer pair LP1195-16Sfor and LP1195-16Srev (Table 1), specific for the *L. paracasei* 1195 16S rRNA gene sequence.

Synthesis of fluorescent cDNA and array hybridization. Procedures for generating fluorescent cDNA probes from purified total bacterial RNA were adapted from protocols of the Brown Laboratory (http://cmgm.stanford.edu/pbrown/protocols/Direct_Label_Protocol1.html). Briefly, 20 μg of total RNA from cells grown on glucose or glucose plus FOS was labeled with Cy3-dCTP fluors (Amersham Biosciences, Piscataway, NJ), whereas 30 μg of RNA from FOS-grown cells was labeled with Cy5-dCTP fluors (Amersham Biosciences) to compensate for the relative inefficiency of Cy5-dCTP incorporation. For each reverse transcription reaction, the mixture of RNA sample with 1 μg of random hexamers (Amersham Biosciences) was adjusted to 14.5 μl, incubated at 65°C for 10 min, and chilled on ice. Six microliters of 5× first-strand buffer (250 mM Tris-HCl, pH 8.3, 375 mM KCl, 15 mM $MgCl_2$) (Invitrogen), 10 mM dithiothreitol (Invitrogen), 0.6 μl of dNTP mix (25 mM of each dATP, dTTP, dGTP, and 10 mM dCTP) (Gibco), 30 U of SUPERase.In (Ambion), and 67 μM of Cy-dCTP fluor dye were then incorporated into each labeling reaction mixture to a final volume of 28 μl. After incubation at 42°C for 2 min, 400 U of Superscript II RNase H^- reverse transcriptase (RT) (Invitrogen) was added, and the reaction mixtures were held at room temperature for 10 min and then incubated at 42°C for 48 min. An additional 200 U of Superscript II was added, and the reaction mixtures were incubated further for 1 h. Finally, transcription reactions were terminated by the addition of EDTA and NaOH, each at a 50 mM final concentration, followed by incubation at 65°C for 30 min to denature the RNA templates. After neutralization with 50 mM (final concentration) HCl, Cy3- and

Cy5-labeled cDNA probes were combined pairwise and purified using QIAquick PCR purification kit columns according to the manufacturer's instructions. The purified probe sample was eluted from the column with 28 μl of ArrayHyb LowTemp hybridization buffer (Sigma) and combined with 550 μg/ml of sheared salmon sperm DNA (Gibco BRL) and 450 μg/ml of yeast tRNA (Sigma) to a final volume of 30 to 32 μl. The resulting probe mixture was incubated at 60°C for 5 min, transferred onto a Hybrislip coverslip (Grace-Biolabs, Inc., Bend, OR), and covered with the array. The slide was incubated in a humidified HybChamber (GeneMachines) in a 48°C water bath for 16 to 20 h. Posthybridized arrays were washed according to procedures described in the ArrayHyb LowTemp hybridization buffer technical bulletin.

Data acquisition and analysis. Comparative hybridization for each experiment was performed in two independent replicates (biological repeats). Hybridized arrays were scanned with a ScanArray 5000 apparatus (Packard Instrument Co., Downers Grove, IL) at 10 μm per pixel resolution. The relative fluorescent intensity of Cy3 and Cy5 for each of the 7,680 features was quantified from TIFF image files (generated by ScanArray 5000) using ImaGene v.4.2 (BioDiscovery, Inc., Marina Del Rey, CA). The fluorescent signal intensities of the array spots for each channel were obtained by subtracting the median intensities of the background pixels from the mean pixel intensities. Global mean normalization of the spot intensities from each channel on individual slides was performed using SNOMAD (http://pevsnerlab.kennedykrieger.org/snomadinput.html). All array data were composited using a Perl-based program, FormatALL (J. Wise and A. K. Benson, unpublished data), yielding the ratio representing the change (*n*-fold) in gene expression levels under FOS conditions (Cy5) relative to gene expression levels with glucose or FOS plus glucose (Cy3). The resulting data were clustered and analyzed using Microsoft Excel (Microsoft Corp., Redmond, WA). Spots for which the ratios for both replicates were less than 2 standard deviations and that had ratios of ≥5 were subjected to further analysis.

DNA sequencing and analysis. Library clones associated with array spots that had an average Cy5/Cy3 transcript ratio of ≥5 were identified, and the inserts were sequenced with vector-specific primers. The sequences were compared against those in the nonredundant protein database using BlastX (http://ncbi.nlm.nih.gov/BLAST). An E value of $\leq 1 \times 10^{-5}$ was set as the cutoff value for the BlastX alignments to be considered relevant. Complete sequences for large inserts that encode genes of interest were obtained by primer walking. All sequences were assembled to contigs using Sequencher v.4.0.5 (Gene Codes Corp., Ann Arbor, MI). Gap sequences between contigs of interest were determined from PCR products amplified from both ends of known sequences. Briefly, PCR products were gel purified and subsequently ligated into the pGEM-T Easy vector (Promega Corp., Madison, WI) according to the manufacturer's recommendations. The ligation products were transformed into *E. coli* DH5α, two independent positive clones containing each cloned PCR product were selected, and inserts were sequenced. Regions flanking the contigs of interest were sequenced by chromosome walking using the tailed-PCR technique as described previously by Rudi et al. (44). Briefly, a single gene-specific primer was used to amplify the region beyond the known sequence with 25 amplification cycles using the Easy-A High-Fidelity PCR cloning enzyme (Stratagene Corp., La Jolla, CA) in a standard 50-μl PCR mixture, which generated a population of single-stranded flanking sequences. The PCR products were purified using a DNA Clean & Concentrator-5 column (Zymo Research) and eluted twice with 6 μl of water. Five microliters of the purified single-stranded PCR products was then used in a 10-μl cytosine tailing reaction mixture containing 1 mM dCTP and 30 U of terminal deoxynucleotidyl transferase (Promega) in 1× terminal deoxynucleotidyl transferase buffer (100 mM cacodylate buffer, pH 6.8, 1 mM $CoCl_2$, 0.1 mM dithiothreitol). The tailing reaction mixture was incubated at 37°C for 20 min followed by enzyme inactivation at 96°C for 4 min. A nested primer in combination with a poly(G) primer complementary to the cytosine tail in the unknown flanking region were then used to amplify the tailed fragments in a standard 50-μl PCR mixture containing 30 pmol of each primer, 2 μl of the tailing products, and 2.5 U of the Easy-A High-Fidelity PCR cloning enzyme. PCR fragments of 1.0 to 1.5 kb were gel purified, ligated into the pGEM-T Easy vector, and cloned into *E. coli* DH5α, and inserts were sequenced as described previously. The tailed-PCR procedures were repeated successively with primers deduced from new sequence data.

Protein sequences were deduced from predicted open reading frames (ORFs) using the JustBio Translator tool (http://www.justbio.com/tools.php), and signal peptides were predicted using SignalP 3.0 (http://www.cbs.dtu.dk/services/SignalP/) (4). Transmembrane helices were identified using Transmembrane TMHMM 2.0 (http://www.cbs.dtu.dk/services/TMHMM/). Sequence alignment was performed using ClustalW (http://www.ebi.ac.uk/clustalw/) under default settings.

RT-PCR analysis for validation of microarray data. For first-strand cDNA synthesis, 5 μg of RNA sample was combined with 0.25 μg of random hexamers in a total volume of 15 μl. The mixtures were incubated at 65°C for 10 min and chilled on ice. Next, 2 μl of 10× StrataScript buffer (0.5 M Tris-HCl, pH 8.3, 0.75 M KCl, 0.03 M $MgCl_2$) (Stratagene), 500 μM dNTP (10 mM each), 20 U of SUPERase.In RNase inhibitor, and 50 U of StrataScript reverse transcriptase (Stratagene) were incorporated into the reaction mixture to a final volume of 20 μl. The reaction mixtures were incubated at room temperature for 10 min, followed by 42°C for 1 h. Reaction mixtures were inactivated at 70°C for 15 min, and RNA templates were hydrolyzed by treatment with 5 U of *E. coli* RNase H (Epicenter Biotechnologies, Madison, WI) for 20 min at 37°C. Target sequences were amplified using 2 μl of cDNA products as a template in standard PCRs for 25 amplification cycles. *L. paracasei* 1195 genomic DNA was used as a PCR template for a positive control. RNA samples without reverse transcription were also included as PCR templates to confirm the absence of contaminating genomic DNA and to verify the results obtained from the amplification of the cDNA products. Semiquantitative analysis of the relative transcript levels of genes associated with the FOS-induced clones was assessed visually by gel electrophoresis.

Construction of the *fosE* insertion mutant. Chromosomal mutation of the *fosE* gene encoding the putative cell wall-associated β-fructosidase was performed by site-directed plasmid integration via homologous recombination (24, 46), with the following modifications. First, a genomic fragment (981 bp) representing an internal region of *fosE* was purified from an *E. coli* shotgun library clone (clone 68G10) (see Table S1 in the supplemental material) by restriction with EcoRI and cloned into the similarly restricted pORI28 integration vector (25). The ligation product was transformed into *E. coli* EC1000 (25), and transformants containing the recombinant plasmid were selected on LB agar containing Kan and Erm. The integrative plasmid, designated pBHE62, was purified and electroporated into *L. paracasei* 1195 cells previously transformed with the pVE6007 helper plasmid, which functions to support the replication of pORI28-based plasmids by providing *repA* in *trans* at 28 to 30°C (26). Transformants carrying the recombinant and helper plasmids were recovered on MRS agar containing 2 μg/ml each of Erm and chloramphenicol after 48 h of incubation at 30°C in ambient atmosphere. A colony was propagated overnight at 30°C in MRS broth (with 5 μg/ml of each antibiotic), and the culture was transferred three times with 1% (vol/vol) inoculum (ca. 30 generations) at 40°C in the presence of Erm (5 μg/ml) only to enrich for cells with chromosomal integration of pBHE62. Insertion mutants that had lost the ability to ferment FOS were selected on mMRS–1% FOS agar medium containing 5 μg/ml Erm and 100 mg/liter bromcresol purple (Fisher). Insertions were confirmed by Southern hybridization of EcoRI-digested genomic DNA from wild-type and mutant strains with a digoxigenin-labeled probe generated from the library clone 68G10 insert fragment using a DIG High Prime DNA Labeling and Detection Starter Kit II (Roche Diagnostics Corp., Indianapolis, IN) according to the manufacturer's instruction. Growth studies of the parent and *fosE* mutant strains were performed by using mMRS broth supplemented with 2% glucose, fructose (Sigma), sucrose (Sigma), FOS, oligofructose (FF_n type) (Orafti North America, Malvern, PA), inulin (Sigma), or 0.5% levan (from *Erwinia herbicola*; Sigma).

Organic acid measurement. Lactic acid and acetic acid were determined using HPLC instrumentation that consisted of a Waters (Milford, MA) 6005 controller, a 717 Plus autosampler adjusted to a temperature of 4°C, and a 996 photodiode array detector. An Aminex ion-exchange column (HPX-87H, 300 by 7.8 mm; Bio-Rad) was equilibrated with 0.008 M sulfuric acid (VWR International, West Chester, PA) at a flow rate of 0.60 ml/min. Each sample was injected onto the column in a 20-μl delivery volume and was resolved under isocratic conditions, with the column temperature maintained at 35°C. Organic acids were identified and quantified by matching the retention times and by evaluating peak areas, respectively, against standards at detection wavelengths of 215 and 230 nm.

Microarray and nucleotide sequence accession numbers. The nucleotide sequences of the *L. paracasei* 1195 *fosRABCDXE* gene cluster and contigs lpca4 to lpca50 have been deposited in GenBank under accession no. DQ396803 and EF030820 to EF030866, respectively. All microarray data are available at the Gene Expression Omnibus (http://www.ncbi.nlm.nih.gov/geo) under accession no. GSE5890.

RESULTS AND DISCUSSION

Shotgun DNA array construction. Based on the reported genome sizes of *Lactobacillus casei* ATCC 334 (http://genome.jgi-psf.org/draft_microbes/lacca/lacca.home.html) and other

TABLE 2. BlastX results for putative FOS-induced contigs

Contig	GenBank accession no.	Top BlastX hit(s)	GenBank accession no. for ortholog	E value	No. of identical amino acids/total no. of amino acids (% identity)
FOS-induced contigs repressed by addition of glucose[a]					
lpca1	DQ396803	β-Fructosidase (fructan hydrolase)	BAD88632	0.00E+00	1,195/1,266 (94)
		β-Phosphoglucomutase	NP_229059	6.00E−14	39/91 (42)
lpca2	DQ396803	LevR protein/transcriptional antiterminator	CAC87264	0.00E+00	442/444 (99)
		LevA protein/PTS mannose/fructose-specific component IIA	CAC87265	2.00E−64	126/126 (100)
lpca3	DQ396803	LevC protein/PTS mannose/fructose/*N*-acetylgalactosamine-specific component IIC	CAF33350	4.00E−111	269/269 (100)
		LevD protein/PTS mannose/fructose/*N*-acetylgalactosamine-specific component IID	ZP_00386224	4.00E−144	282/283 (99)
		Hypothetical protein (putative PTS component)	ZP_00386223	5.00E−46	109/110 (99)
lpca4	EF030820	Permease of major facilitator superfamily	ZP_00384423	3.00E−106	202/204 (99)
		PTS mannose/fructose/*N*-acetylgalactosamine-specific component IIB	ZP_00384422	0.00E+00	324/324 (100)
		PTS mannose/fructose/*N*-acetylgalactosamine-specific component IIC	ZP_00384421	4.00E−51	151/153 (98)
		PTS mannose/fructose/*N*-acetylgalactosamine-specific component IID	ZP_00384420	2.00E−117	207/207 (100)
lpca5	EF030821	Transcriptional regulator	ZP_00385283	1.00E−33	76/76 (100)
		PTS mannose/fructose/*N*-acetylgalactosamine-specific component IIB	ZP_00385284	4.00E−86	164/168 (97)
		PTS mannose/fructose/*N*-acetylgalactosamine-specific component IIC	ZP_00385285	5.00E−85	180/180 (100)
		PTS mannose/fructose/*N*-acetylgalactosamine-specific component IID	ZP_00385286	1.00E−135	258/266 (97)
		Putative α-glucosidase	ZP_00385287	1.00E−29	65/68 (95)
lpca6	EF030822	PTS fructose-specific component IIC	ZP_00384705	3.00E−80	179/179 (100)
		Fructose-1-phosphate kinase and related fructose-6-phosphate kinase (PfkB)	ZP_00384706	5.00E−111	204/211 (96)
		Transcriptional regulator of sugar metabolism	ZP_00384707	2.00E−86	166/172 (96)
lpca7	EF030823	SipD (similar to EIID-mannose, a new mannose-like PTS from *L. casei* controlled by a PRD^b-containing regulator and σ^{54})	AAR89080	3.00E−55	117/249 (46)
lpca8	EF030824	ABC-type uncharacterized transport system, periplasmic component	ZP_00385071	9.00E−100	191/194 (98)
lpca9	EF030825	α-Galactosidase	ZP_00385829	2.00E−106	361/363 (99)
lpca10	EF030826	*N*-Acetyl-β-hexosaminidase	ZP_00384988	0.00E+00	361/369 (97)
lpca11	EF030827	Galactose mutarose-related enzymes	ZP_00386133	1.00E−105	184/187 (98)
lpca12	EF030828	Transcriptional antiterminator *licT*	NP_347062	2.00E−26	66/199 (33)
lpca13	EF030829	Transcriptional antiterminator	ZP_00385530	2.00E−45	298/308 (97)
lpca14	EF030830	Transcriptional regulator	ZP_00385986	4.00E−54	110/113 (97)
		2-Keto-3-deoxy-6-phosphogluconate aldolase	ZP_00385987	8.00E−118	216/216 (100)
lpca15	EF030831	5-Keto-4-deoxyuronate isomerase	ZP_00384854	4.00E−111	191/193 (98)
		Dehydrogenase with different specificities (related to short-chain alcohol dehydrogenases)	ZP_00384855	4.00E−119	218/220 (99)
		Sugar kinase (ribokinase family)	ZP_00384856	2.00E−123	176/178 (98)

Continued on facing page

TABLE 2—*Continued*

Contig	GenBank accession no.	Top BlastX hit(s)	GenBank accession no. for ortholog	E value	No. of identical amino acids/total no. of amino acids (% identity)
lpca16	EF030832	Dehydrogenase with different specificities (related to short-chain alcohol dehydrogenases)	ZP_00385575	7.00E−107	188/189 (99)
lpca17	EF030833	Pyruvate/2-oxoglutarate dehydrogenase complex, dehydrogenase (E1) component, α subunit	ZP_00384286	2.00E−154	284/284 (100)
		Pyruvate/2-oxoglutarate dehydrogenase complex, dehydrogenase (E1) component, β subunit	ZP_00384287	2.00E−153	295/297 (99)
lpca18	EF030834	Pyruvate/2-oxoglutarate dehydrogenase complex, dihydrolipoamide acyltransferase (E2) component	ZP_00384288	5.00E−113	331/364 (90)
		Pyruvate/2-oxoglutarate dehydrogenase complex, dihydrolipoamide dehydrogenase (E3) component	ZP_00384289	0.00E+00	464/467 (99)
lpca19	EF030835	Pyruvate formate-lyase	ZP_00384135	6.00E−82	362/400 (91)
lpca20	EF030836	Putative NADH oxidase	NP_785464	9.00E−74	139/279 (49)
lpca21	EF030837	Phosphoribosyl-dephospho-CoA[c] transferase (holo-ACP synthetase)	ZP_00385601	6.00E−52	117/119 (98)
		Citrate lyase, α subunit	ZP_00385602	0.00E+00	448/453 (98)
		Citrate lyase, β subunit	ZP_00385603	1.00E−144	282/285 (98)
		Citrate lyase synthetase	ZP_00385605	3.00E−154	300/305 (98)
		Na^+-transporting methylmalonyl-CoA/oxaloacetate decarboxylase, β subunit	ZP_00385606	7.00E−81	159/161 (98)
lpca22	EF030838	ATPase related to helicase subunit of Holliday junction resolvase	ZP_00385394	2.00E−157	286/289 (98)
		Acetate kinase	ZP_00385393	1.00E−92	175/177 (98)
lpca23	EF030839	Threonine dehydratase	ZP_00386338	6.00E−162	291/295 (98)
		Predicted membrane protein	ZP_00386337	2.00E−89	226/229 (98)
lpca24	EF030840	Hypothetical protein	ZP_00385174	2.00E−107	194/196 (98)
FOS-induced contigs not repressed by addition of glucose[d]					
lpca25	EF030841	PTS cellobiose-specific component, IIA	ZP_00384630	3.00E−51	105/105 (100)
		PTS cellobiose-specific component, IIB	ZP_00384343	5.00E−35	76/101 (75)
		PTS cellobiose-specific component, IIC	ZP_00384631	2.00E−147	282/283 (99)
		β-Glucosidase/6-phospho-β-glucosidase/β-galactosidase	ZP_00384632	0.00E+00	386/429 (89)
		Transcriptional regulator	ZP_00384633	3.00E−87	163/164 (99)
lpca26	EF030842	PTS IIC component	AAO81603	8.00E−80	173/244 (70)
lpca27	EF030843	PTS IIC component, glucose/maltose/*N*-acetylglucosamine-specific	ZP_00384211	1.00E−45	93/93 (100)
		Glycosidase	ZP_00384212	2.00E−104	177/188 (94)
lpca28	EF030844	BglG family transcriptional antiterminator	BAD63396	1.00E−12	34/78 (43)
		Putative fructose-bisphosphate aldolase	BAD63397	1.00E−34	70/110 (63)
		PTS fructose-specific enzyme IIBC component	BAD63398	7.00E−41	86/184 (46)
lpca29	EF030845	ABC-type multidrug transport system, ATPase and permease components	ZP_00385291	2.00E−122	240/247 (97)
lpca30	EF030846	Transcriptional antiterminator	ZP_00385530	2.00E−89	170/171 (99)
lpca31	EF030847	Predicted transcriptional regulator	ZP_00385948	7.00E−36	75/76 (98)
		3-Methyladenine DNA glycosylase	ZP_00385950	4.00E−107	192/193 (99)

Continued on following page

TABLE 2—*Continued*

Contig	GenBank accession no.	Top BlastX hit(s)	GenBank accession no. for ortholog	E value	No. of identical amino acids/total no. of amino acids (% identity)
lpca32	EF030848	Pyruvate/2-oxoglutarate dehydrogenase complex, dihydrolipoamide dehydrogenase (E3) component and related enzymes	ZP_00386162	2.00E−124	236/238 (99)
lpca33	EF030849	Uncharacterized NAD(FAD)-dependent dehydrogenase	ZP_00385517	2.00E−103	185/188 (98)
lpca34	EF030850	Putative pyruvate oxidase	ZP_00322361	4.00E−82	384/481 (80)
lpca35	EF030851	Alanine dehydrogenase Dehydrogenase with different specificities (related to short-chain alcohol dehydrogenases)	ZP_00386339 ZP_00385842	9.00E−163 1.00E−122	312/314 (99) 218/220 (99)
lpca36	EF030852	Orotate phosphoribosyltransferase Transposase and inactivated derivatives	ZP_00386110 ZP_00385279	2.00E−44 3.00E−52	91/92 (99) 116/130 (89)
lpca37	EF030853	DNA replication protein	ZP_00385903	1.00E−123	224/247 (90)
lpca38	EF030854	Nucleotidyltransferase/DNA polymerase involved in DNA repair Acetyl-CoA carboxylase, α and β subunits	ZP_00386051 ZP_00386052	4.00E−60 7.00E−56	113/115 (98) 105/106 (99)
lpca39	EF030855	Putative ADP-ribosylglycohydrolase	NP_346980	1.00E−38	90/219 (41)
lpca40	EF030856	Putative transposase Hypothetical protein	NP_604416 AAW81273	3.00E−44 4.00E−49	93/95 (97) 97/153 (63)
lpca41	EF030857	Conserved hypothetical protein	ZP_00384901	0.00E+00	356/363 (98)
lpca42	EF030858	Hypothetical protein	ZP_00385610	4.00E−23	64/64 (100)
lpca43	EF030859	Hypothetical protein	ZP_00386503	9.00E−06	40/40 (100)
lpca44	EF030860	Hypothetical protein	ZP_00385356	9.00E−51	102/103 (99)
lpca45	EF030861	Putative dehydrogenase Hypothetical protein	ZP_00385097 ZP_00385096	3.00E−80 5.00E−16	153/157 (97) 46/47 (97)
lpca46	EF030862	Hypothetical protein	AAW81265	1.00E−16	45/75 (60)
lpca47	EF030863	No hit			
lpca48	EF030864	No hit			
lpca49	EF030865	No hit			
lpca50	EF030866	No hit			

[a] Contigs that were differentially expressed in hybridization experiments with both FOS versus glucose and FOS versus FOS plus glucose. Contigs lpca1 to lpca3 are parts of the putative *fos* gene cluster.
[b] PRD, PTS regulation domain.
[c] CoA, coenzyme A.
[d] Contigs that were differentially expressed in the hybridization experiment with FOS versus glucose only.

sequenced *Lactobacillus* strains (1, 8, 23, 42, 49), we predicted that *L. paracasei* 1195 has a genome size of approximately 2.0 to 2.5 Mb. Hence, the constructed shotgun DNA array of the 7,680 clones provided approximately five times coverage of the *L. paracasei* genome [(average PCR product size of 1,500 bp × 7,680 clones)/predicted genome size of 2.5×10^6 bp].

Induction of genes during growth on FOS compared to glucose. In order to identify genes involved in the utilization of FOS by *L. paracasei*, the differential transcription profiles between cells grown with FOS and those grown in glucose as the sole carbon source were examined. Compared to cells supplemented with glucose, the growth of cells in the presence of FOS resulted in fivefold or greater induction in 117 array features (see Table S1 in the supplemental material), or about 1.5% of the clones represented on the array. Of these clones, 48% (56/117) exhibited 10-fold or more induction. Subsequent sequencing and contig analysis of the 117 FOS-inducible clones from this experiment revealed 50 independent contigs (contigs lpca1 to lpca50) (Table 2).

Based on BlastX analysis, most (37 contigs) of the 50 FOS-

induced contigs encoded proteins with orthologs in the *L. casei* neotype strain, strain ATCC 334. Among the contigs that were differentially expressed, one (lpca1) had significant sequence identity to a fructan hydrolase (GenBank accession no. BAD88632) (94% identity) and a β-fructosidase (accession no. ZP_00386222) (71% identity) from an unassigned strain of *L. casei* and from *L. casei* ATCC 334, respectively. Another induced contig (lpca3) encoded transport function proteins, including structural components of PTS apparently related to the transport of fructose. Most of these PTS components also showed strong identity to the levanase (*lev*)-PTS encoded by the *levRABCDX* gene cluster from *L. casei* BL23 (28) and the mannose/fructose-specific PTS (accession no. ZP_00386224 to ZP_00386227) encoded in a putative levanase operon in *L. casei* ATCC 334. Interestingly, the transcriptional levels of contigs encoding putative sugar transport and catabolic functions unrelated to β-fructosides or its constituents, such as those encoding α-galactosidase (lpca9), *N*-acetyl-β-hexosaminidase (lpca10), galactomutarotase (lpca11), β-glucosidase, and cellobiose-specific PTS (lpca25), were also higher during growth on FOS than during growth on glucose. Whether this is a consequence of coregulation or due to proximity to the FOS-induced genes remains to be determined.

Expression of several other genes encoding proteins with sequence identity to metabolic enzymes, including putative fructose-1-phosphate kinase (lpca6), fructose-bisphosphate aldolase (lpca28), pyruvate dehydrogenase subunits (lpca17, lpca18, and lpca32), NADH oxidase (lpca20), citrate lyase (lpca21), and alanine dehydrogenase (lpca35), was also elevated during growth on FOS. Ten of the FOS-induced contigs encode proteins that shared sequence identity to transcriptional regulators, five of which were transcriptional antiterminators. In particular, lpca2 encodes part of a putative protein that shows sequence identity to a LevR transcriptional antiterminator from *L. casei* BL23 and *L. casei* ATCC 334. Unlike the LevR of the levanase operon in *Bacillus subtilis*, however, the LevR from BL23 is not σ^{54} regulated (28). Four of the gene sequence queries yielded no matches from the database (lpca47 to lpca50) and were therefore assigned as hypothetical proteins. Finally, in contrast to cells grown in the presence of FOS versus glucose, there were few differences in the expression profiles of cells grown in the presence FOS or fructose (see Table S1 in the supplemental material), suggesting that fructose is an apparent inducer of genes involved in FOS utilization.

Repression of FOS genes by glucose. When glucose was added to mid-logarithmic-phase FOS-grown cells, transcription of nearly half (24 contigs) of the 50 FOS-induced contigs (lpca1 to lpca24) (Table 2) representing 97 clones (see Table S2 in the supplemental material) was repressed. Among these contigs are those that encode the previously described β-fructosidase, structural components of putative fructose PTS, transcriptional antiterminators, several non-β-fructoside-related catabolic enzymes (lpca9 to lpca11), and enzymes involved in pyruvate metabolism (lpca17 to lpca22). These results indicate that some of the genes that are FOS induced are subject to some type of catabolite regulation. Meanwhile, the remaining 26 FOS-induced contigs (lpca25 to lpca50) (Table 2) are likely not glucose regulated. Thus, there are at least two classes of FOS-induced genes that are regulated independently. Several of these contigs that were not repressed by glucose correspond to genes encoding PTS transporters specific for glucosides and fructose (lpca25 to lpca28). Unlike the pyruvate metabolic enzymes encoded by contigs lpca17 to lpca 22, the expression of lpca32 to lpca35, which code for putative pyruvate oxidase, the dihydrolipoamide dehydrogenase (E3) component of the pyruvate dehydrogenase complex, alanine dehydrogenase, and a NADH oxidase, appeared to be unaffected by glucose. Furthermore, over one-third (11) of the contigs (lpca40 to lpca50) code for an uncharacterized conserved protein and hypothetical proteins. Interestingly, genes encoding the orthologs of lpca41 and lpca44 in *L. casei* ATCC 334 are located downstream and in between genes encoding components of putative fructose PTS, respectively. We also detected contigs that were down-regulated in response to the addition of glucose to mid-logarithmic-phase FOS-grown cells but that were not differentially expressed between cells induced with FOS or glucose during the 30-min induction period (data not shown).

Validation of microarray data by RT-PCR analysis. To validate the expression data obtained from the array hybridization experiments, RT-PCR experiments were used to measure mRNA levels from genes of interest. Primers specific for three of the FOS-induced clones (Table 1) were used to amplify the corresponding cDNA products generated from RNA of cells grown on FOS, glucose, fructose, FOS plus glucose, or FOS plus fructose. Figure 1 shows the RT-PCR products for three specific clones, corresponding to a segment of contig lpca3 encoding components IIC and IID of a putative fructose PTS and two different segments of contig lpca1 encoding a putative FOS hydrolase (β-fructosidase). Visual inspection of the stained band intensities resulting from gel electrophoresis of the RT-PCR products showed a strong correlation between the relative band intensities and their expression levels in the different growth conditions observed in the array analysis. All three clones were induced in FOS- and fructose-grown cells but not in glucose-grown cells. In addition, a reduction in the accumulated transcripts from the three clones was observed when glucose was added to the FOS-grown cells. Thus, our RT-PCR data are consistent with the data obtained from the microarray experiments. Interestingly, we observed that unlike glucose, fructose did not cause catabolite repression of transcription from lpca1 or lpca3, since no measurable difference in the transcript levels was observed for FOS-grown cells with the addition of fructose or fructose-grown cells compared to FOS-grown cells. Therefore, fructose does not result in catabolite repression at these loci, as does glucose. Similarly, expression of the *bfrA* gene in *L. acidophilus* NCFM, coding for an FOS-hydrolyzing fructosidase, was also not affected by fructose (3). The 16S rRNA gene served as a housekeeping gene, and no measurable difference in band intensities was observed under all conditions.

Identification of a conserved putative sugar operon involved in FOS utilization. Contigs lpca2 to lpca6 encode PTS that are potentially involved in the transport of fructose. Contigs lpca2 and lpca3, in particular, exhibit a structural organization similar to that of the *levRABCDX* gene cluster from *L. casei* BL23 (28) (Fig. 2B). The *levABCDX* operon was shown to be induced by fructose and mannose, and expression of the operon was regulated by the LevR transcriptional activator encoded by the *levR* gene transcribed divergently from the operon (28). In

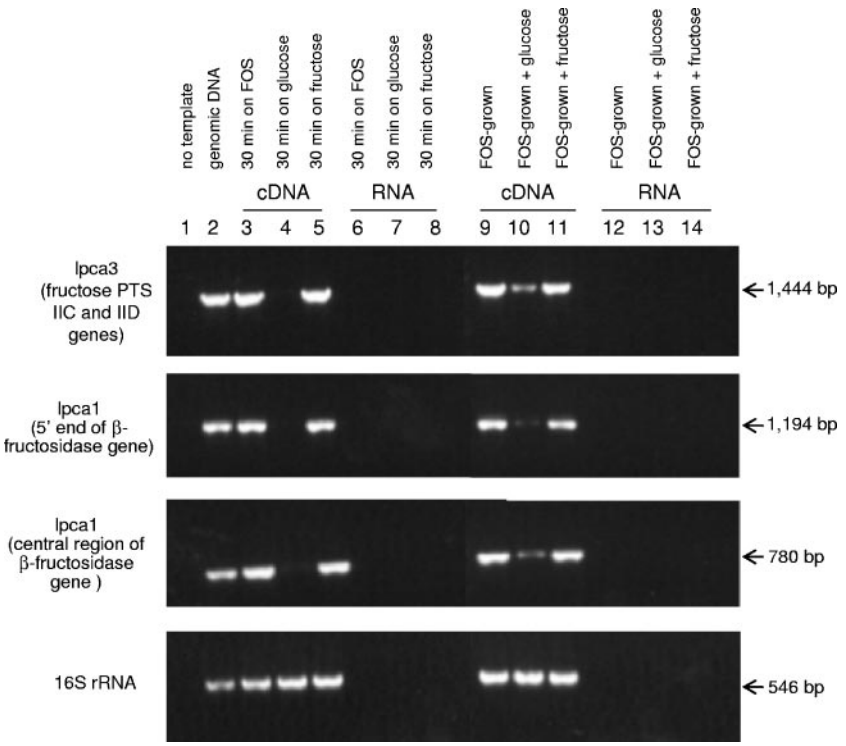

FIG. 1. Differential expression analysis of FOS-induced genes in *Lactobacillus paracasei* 1195 by RT-PCR. Semiquantitative RT-PCR analysis was used to confirm the transcription of genes corresponding to contigs lpca3 and lpca1. Cells were grown and harvested as follows: lane 1, PCR negative control (no template); lane 2, *L. paracasei* 1195 genomic DNA as a PCR template (positive control); lanes 3 and 6, 30 min of growth on FOS; lanes 4 and 7, 30 min of growth on glucose; lanes 5 and 8, 30 min of growth on fructose; lanes 9 and 12, FOS-grown cells; lanes 10 and 13, FOS-grown cells with glucose added; lanes 11 and 14, FOS-grown cells with fructose added.

present study, the expression analysis in which the transcriptional profiles of FOS-grown cells and fructose-grown cells were compared demonstrated that the genes encoding the putative fructose PTS components were not differentially expressed (see Table S1 in the supplemental material). These results implied that the fructose PTS encoded by contigs lpca2 and lpca3 was also induced by fructose, possibly in a fashion similar to that of the *levABCDX* operon (28). Contigs lpca2 and lpca3 along with lpca1 all aligned to nonoverlapping portions of the putative levanase operon in *L. casei* ATCC 334 (LcasA01000257 to LcasA01000263), which consists of genes encoding a fructose/mannose PTS and a cell wall-anchored β-fructosidase precursor. It is therefore likely that these contigs are actually part of a single genetic locus that is responsible for the hydrolysis of FOS and the subsequent uptake of the hydrolyzed products (consisting mainly of fructose) (7, 30, 39). It is notable that putative fructose PTS transporters encoded by three other contigs, lpca4, lpca5, and lpca6, were also upregulated during FOS utilization. Presumably, their function is also to accumulate fructose monomers released by the β-fructosidase.

Contig lpca1 consists of the partial gene sequence encoding a putative β-fructosidase. Included at the C-terminal region is a putative gram-positive bacteria cell wall anchor motif, LPQAG (35), followed by a hydrophobic domain and a short tail of positively charged residues. Similar cell wall sorting signals are also present in the C termini of the β-fructosidase homologs from *L. casei* ATCC 334 (LPKTG) (GenBank accession no. ZP_00386222) and the fructan hydrolase from another strain of *L. casei* (LPQAG) (accession number BAD88632). In addition, signal peptidase cleavage sites were present at the N-terminal regions of both of these *L. casei* β-fructosidases as well as in the *L. paracasei* 1195 β-fructosidase (which will be discussed below). These observations suggest that this putative β-fructosidase in *L. paracasei* 1195 is cell wall associated and that it hydrolyzes FOS extracellularly.

Characterization of the putative *fos* utilization cluster. (i) Gene organization. To confirm our hypothesis that lpca1 to lpca3 are derived from a single *fos* locus, gap sequences and flanking regions of lpca1 to lpca3 were determined by PCR and chromosome walking. Analysis of the 12,219-bp chromosomal region revealed the presence of seven putative ORFs (Fig. 2A). The cluster consists of genes encoding a transcriptional regulator (*fosR*); the EIIA, IIB, IIC, and IID components of a fructose/mannose-specific PTS (*fosABCD*); a hypothetical protein (*fosX*); and a β-fructosidase (*fosE*). In addition to having extensive similarity to the putative levanase operon of *L. casei* ATCC 334, the structural organization and gene sequence of the *fos* operon are also highly similar to those of the levanase-PTS operons of *L. casei* BL23, *Bacillus subtilis* 168, *Bacillus licheniformis* DSM 13/ATCC 14580, and *Clostridium acetobutylicum* ATCC 824 (Fig. 2B).

(ii) Coexpression of the *fos* genes. To determine whether the FOS genes were cotranscribed as a single polycistronic mRNA, cDNA products generated from total RNA extracted from cells induced by FOS were used as PCR templates in RT-PCRs

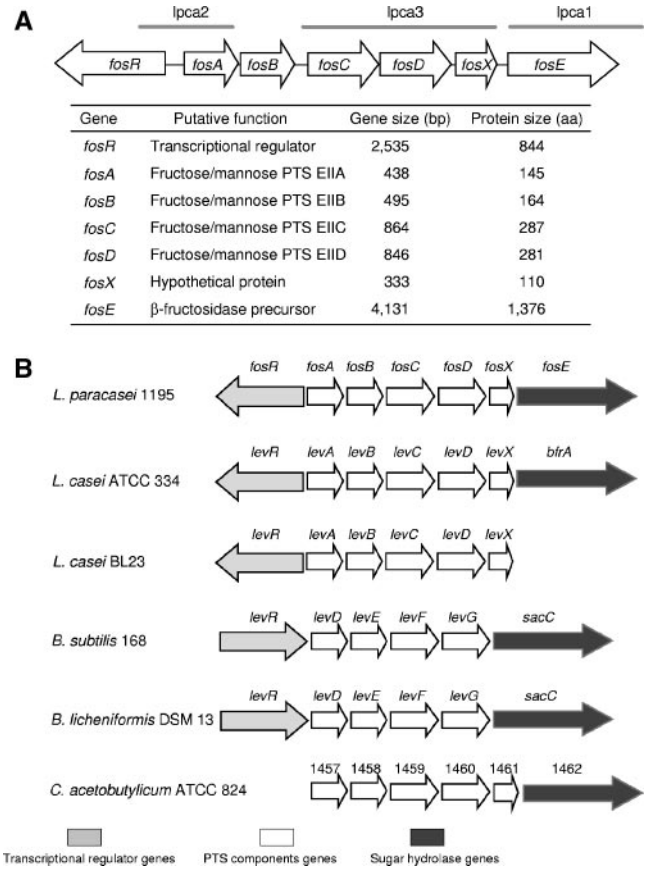

Gene	Putative function	Gene size (bp)	Protein size (aa)
fosR	Transcriptional regulator	2,535	844
fosA	Fructose/mannose PTS EIIA	438	145
fosB	Fructose/mannose PTS EIIB	495	164
fosC	Fructose/mannose PTS EIIC	864	287
fosD	Fructose/mannose PTS EIID	846	281
fosX	Hypothetical protein	333	110
fosE	β-fructosidase precursor	4,131	1,376

FIG. 2. (A) Gene organization of the putative FOS utilization gene cluster in *Lactobacillus paracasei* 1195. Positions of contigs lpca1 to lpca3 corresponding to the *fos* gene cluster are indicated. (B) Comparison of the structural organization of the *fos* gene cluster and the levanase or levanase-like operons in related organisms.

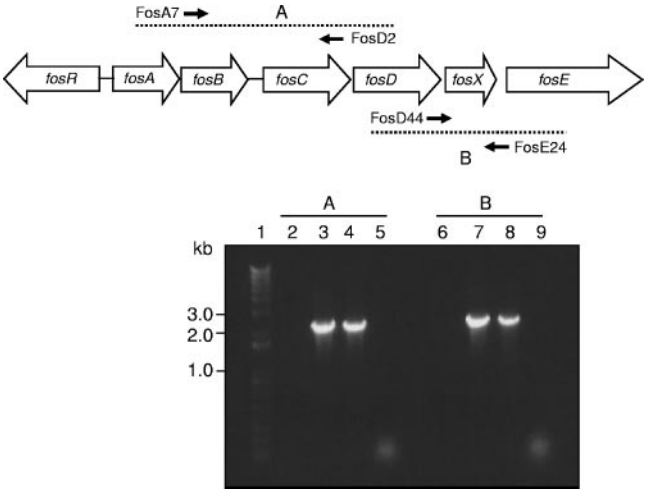

FIG. 3. Coexpression of *fos* genes. Primer pairs FosA7-FosD2 and FosD44-FosE24 were used to amplify regions spanning *fosA-fosD* (A) and *fosD-fosE* (B), respectively. Dotted lines represent the regions of amplification. Lane 1, 0.25 μg of 1 Kb Plus DNA Ladder (Invitrogen); lanes 2 and 6, PCR negative control; lanes 3 and 7, *L. paracasei* 1195 genomic DNA as a PCR template; lanes 4 and 8, cDNA generated from FOS-induced *L. paracasei* 1195 cells as a PCR template; lanes 5 and 9, 5 μg of total RNA from FOS-induced cells without RT as a PCR template.

to test for the amplification of overlapping regions spanning the *fosA-fosD* genes and the *fosD-fosE* genes. Only a single PCR product was obtained from each amplification reaction using the FosA7-FosD2 or FosD44-FosE24 primer pair (Fig. 3). The PCR product sizes for *fosA-D* and *fosD-E*, as estimated from the complete sequence of the putative operon, were 2,274 bp and 2,449 bp, respectively, which correspond to the approximate sizes of PCR bands observed on the gel. These results were confirmed in three replicated experiments using independent RNA samples and are consistent with the notion that the *fosABCDXE* genes are cotranscribed as an operon.

(iii) Sequence analysis of the *fos* gene cluster. The 2,535-bp putative *fosR* gene is the first ORF in the gene cluster that precedes the operon and is oriented in the opposite direction from the other ORFs. The deduced amino acid sequence of FosR exhibits 99% identity to both the LevR transcriptional regulator of *L. casei* BL23 and a putative transcriptional antiterminator encoded upstream of the putative levanase operon in *L. casei* ATCC 334. These transcriptional regulators belong to a family of multidomain regulators that contain (a) a DNA-binding domain with a helix-turn-helix motif at the N-terminal region, (b) a domain similar to the central domain of NifA/NtrC family positive regulators, and (c) two EII domains, EIIA and EIIB, located between two PTS regulation domains at the center and C-terminal part of the protein (28). The domain organization of these transcriptional regulators shares similarity to that of the σ^L-dependent LevR transcriptional activator of *B. subtilis* (GenBank accession no. NP_390586) (9, 28), although there is only 23% amino acid sequence identity between these proteins and the LevR of *B. subtilis*.

The first four structural genes of the *fosABCD* operon encode the EIIABCD components of the fructose/mannose PTS. The intergenic regions of *fosR-fosA* and *levR-levA* in *L. casei* BL23 (28) are nearly identical, with only a single nucleotide difference at position 37 upstream of the *fosR*. A putative *cre* sequence, ATTGTAAGCGTTAACCTT, that differs from the consensus sequence, also by only 1 base (29), is located at nucleotide positions 184 to 201 upstream from both the *levA* (28) and *fosA* genes. The deduced FosABCD polypeptides shared more than 99% identity to the corresponding proteins in both *L. casei* BL23 and ATCC 334 and 23 to 62% sequence identity to the corresponding components of the *lev* operons in *B. subtilis* 168 and *C. acetobutylicum* ATCC 824. Analysis of the deduced protein sequences predicted that FosA and FosB are cytoplasmic proteins that are presumably responsible for the phosphorylation of the substrates, whereas FosC and FosD are membrane-bound permease components that are likely specific for fructose and/or mannose. The *fosX* gene encodes a 110-residue hypothetical protein that contains two predicted transmembrane helices between amino acid residues 24 and 46 and between amino acid residues 50 and 72. This hypothetical integral membrane protein shared 99% identity with a hypothetical protein and the LevHX1 protein from *L. casei* ATCC 334 (GenBank accession no. ZP_00386223) and an *L. casei* strain (accession no. BAD88631), respectively; 96% sequence identity with the LevX protein of *L. casei* BL23 (accession no. CAF33352); and 58% and 50% identity to a hypothetical pro-

tein from *Lactobacillus johnsonii* NCC 533 (accession no. NP_965459) and *Streptococcus mutans* UA159 (accession no. AAN59563), respectively. In all cases, the orthologs of FosX are located downstream of mannose/fructose EIID genes. Interpretation of the BlastX data suggests that these small putative PTS proteins are conserved within the lactic acid bacteria, since no orthologs were found in other bacteria.

The 4,131-bp *fosE* gene, encoding the β-fructosidase enzyme precursor, is the distal gene of the *fos* gene cluster and is located 206 bp downstream from the termination codon of *fosX*. No apparent −10 and −35 promoter elements were detected within the *fosX-fosE* intergenic region, nor were −12 or −24 promoter elements found upstream of *fosE* or *fosR*. The FosE protein exhibits significant sequence identity (70 to 90%) to the fructan hydrolase (LevH1) (GenBank accession no. BAD88632) of an *L. casei* strain and the β-fructosidase (BfrA) (accession no. ZP_00386222) from the putative levanase operon of *L. casei* ATCC 334. Alignment of the FosE protein sequence with LevH1 and BfrA confirmed that the FosE and LevH1 proteins were more closely related to each other than to BfrA (see Fig. S1 in the supplemental material). On the other hand, FosE shares only moderate sequence identity (31 to 32%) with the levanases from *B. subtilis* 168 (accession no. NP_390581) and *B. licheniformis* DSM 13 (accession no. AAU41697), with the identity confined to the central region of FosE. Regardless of the differences, these β-fructosidases contain motifs that are conserved in glycosyl hydrolase family 32 as well as the putative amino acid residues essential for the catalytic activity (34, 41).

A signal peptidase cleavage site was predicted between amino acid residues 40 and 41 of the deduced FosE protein sequence (see Fig. S1 in the supplemental material). As indicated previously, the enzyme contains gram-positive cell wall sorting signals that include the signature motif LPQAG (consensus sequence of LPx[T/A]G), followed by a hydrophobic domain and a short positively charged tail at the C-terminal region (35). Close inspection of the FosE protein sequence revealed the presence of six imperfect copies of repeat sequences of ca. 80 amino acids in length, starting at position Ala-825 and extending towards the C-terminal region of the precursor protein (see Fig. S1 in the supplemental material). Similar sequence repeats were also found in LevH1 of *L. casei* but not in BfrA of strain ATCC 334. Based on BlastP searches, these sequence repeats of unknown function are also present in multiple copies in various cell surface proteins and putative peptidoglycan-bound proteins from *Lactobacillus plantarum* (GenBank accession no. NP_784544 and NP_786170), *Listeria monocytogenes* (accession no. EAL10229 and NP_464368), *Listeria innocua* (accession no. NP_470145), and *Enterococcus faecalis* (accession no. AAO82221). This observation suggests that these repeats may serve an important role in the association of the proteins with the cell wall peptidoglycan in gram-positive microorganisms.

Overall, the high degree of conservation observed among the *lev* clusters in both *L. casei* ATCC 334 and BL23 and the *fos* cluster of *L. paracasei*, in terms of sequence similarity and operon architecture, suggested that the gene clusters may have originated from a common ancestor. The major difference is the absence of a β-fructosidase-encoding gene in the *lev* cluster of *L. casei* BL23. It has been proposed that gene rearrangement events in *L. casei* BL23 may have caused the separation of the β-fructosidase-encoding gene from the *lev* operon (28). Meanwhile, the difference between FosE and BfrA of *L. casei* ATCC 334, particularly the predicted sizes of both proteins and the variations in their C-terminal region sequences, suggests that these enzymes may have evolved independently. It is noteworthy that the *levH1* gene encoding LevH1 in the undesignated *L. casei* strain is located downstream of *levHX1*, which encodes a protein similar to FosX. Therefore, it is plausible that the *levHX1-levH1* gene cluster represents the distal region of a *fos*-like operon in this *L. casei* strain.

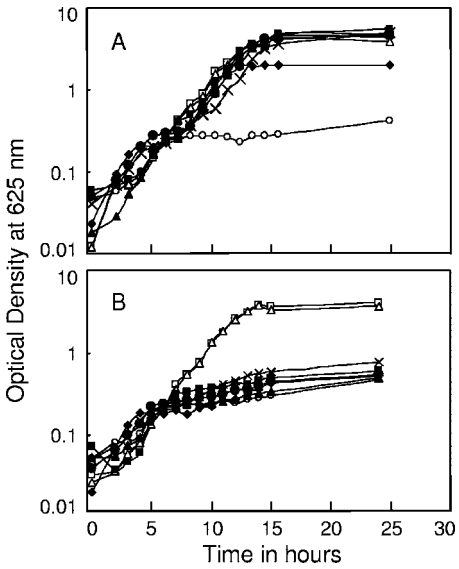

FIG. 4. Growth of *Lactobacillus paracasei* 1195 (A) and its isogenic *fosE* mutant strain (B) in mMRS medium containing no added carbohydrate (○), glucose (□), fructose (△), sucrose (×), FOS (●), oligofructose (■), inulin (▲), and levan (◆). All carbohydrates were added at 2%, except levan, which was added at 0.5%.

Insertional inactivation of *fosE* affects growth on β-fructose-linked sugars. To confirm the essential role of *fosE* in FOS metabolism, a mutation was introduced into *L. paracasei* 1195, and growth of this *fosE* mutant strain was compared to that of the parental strain (Fig. 4). Although the wild-type strain grew well on all of the substrates, the *fosE* mutant strain was able to reach high cell densities only when grown in media containing glucose or fructose. Growth on sucrose, FOS, oligofructose (FF_n type), inulin, and levan was essentially indistinguishable from that of cells grown in the absence of an added carbohydrate. Therefore, the functional activity of the FosE protein was required for growth on β-fructose-linked substrates.

FOS metabolism in *L. paracasei*. After a 30-min induction period, cells induced by FOS appeared to express higher levels of metabolic enzymes involved in pyruvate metabolism (lpca17 to lpca22) (Table 2) than cells grown on glucose. Indeed, in one recent study (27), it was reported that *Lactobacillus paracasei* subsp. *paracasei* 8700:2 produced acetate, formate, and ethanol during growth on oligofructose (of the FF_n type), whereas growth on fructose yielded only lactic acid. However, when *L. paracasei* 1195 was grown in mMRS broth containing FOS, glucose, or fructose, lactic acid was the only product that was detected by HPLC analysis of culture broths (data not

shown). Thus, it appears that FOS was utilized, like glucose and fructose, via homofermentative metabolism.

Previous transport and enzyme assays suggested that *L. paracasei* 1195 accumulated FOS via an ABC transporter and that hydrolysis of FOS was catalyzed by a cytoplasmic β-fructosidase (22). In the present study, it was expected that genes encoding an ABC transporter and an intracellular β-fructosidase would be identified from the transcriptional profiles of *L. paracasei* 1195 grown on FOS. However, based on expression analysis, no induction of genes encoding components of a sugar ABC transporter was detected when cells were grown on FOS. Moreover, none of the FOS-induced genes identified showed similarity to sucrose phosphorylase, fructokinase, or glucokinase, which are required to metabolize intracellular FOS hydrolysis products. Instead, the identification of a putative cell wall-associated β-fructosidase by array expression profiling (Table 2) suggested that FOS may be hydrolyzed into fructose and sucrose extracellularly by the β-fructosidase and that uptake of these molecules is subsequently mediated by fructose and sucrose PTS as discussed above. The increased expression of genes encoding the fructose PTS transporter and 1-phosphofructokinase in FOS-induced cells would provide rapid uptake and utilization of fructose as an energy source. In a recent study, Makras et al. (27) showed that *L. paracasei* subsp. *paracasei* 8700:2 grew rapidly on inulin and oligofructose and that hydrolysis was extracellular. In contrast, FOS hydrolysis activity in *L. paracasei* 1195 was absent in the supernatant and intracellular extract but was present in the cell wall fraction (data not shown). Nevertheless, functional analysis of the putative FOS operon is under way to establish its role in the metabolism of FOS by *L. paracasei* 1195.

ACKNOWLEDGMENTS

This study was supported, in part, by a grant from Dairy Management Inc. This paper is a contribution of the University of Nebraska Agricultural Research Division, supported in part by funds provided through Hatch Act funds, USDA.

We thank the Joint Genome Institute of the U.S. Department of Energy for providing access to the *Lactobacillus casei* ATCC 334 draft genome, Jennifer Huebner for technical assistance, Min Zhang for technical advice on the microarray hybridizations, and Stephen D. Kachman for advice on data analysis. We also thank E. Maguin for providing pVE6007, T. Klaenhammer for providing pORI28 and *E. coli* EC1000, and J. Broadbent for sharing a partial sequence from the *L. casei* ATCC 334 genome.

REFERENCES

1. **Altermann, E., W. M. Russell, M. A. Azcarate-Peril, R. Barrangou, B. L. Buck, O. McAuliffe, N. Souther, A. Dobson, T. Duong, M. Callanan, S. Lick, A. Hamrick, R. Cano, and T. R. Klaenhammer.** 2005. Complete genome sequence of the probiotic lactic acid bacterium *Lactobacillus acidophilus* NCFM. Proc. Natl. Acad. Sci. USA **102:**3906–3912.
2. **Bailey, J. S., C. Blankenship, and N. A. Cox.** 1991. Effect of fructooligosaccharide on *Salmonella* colonization of the chicken intestine. Poult. Sci. **70:** 2433–2438.
3. **Barrangou, R., E. Altermann, R. Hutkins, R. Cano, and T. R. Klaenhammer.** 2003. Functional and comparative genome analyses of an operon involved in fructooligosaccharide utilization by *Lactobacillus acidophilus*. Proc. Natl. Acad. Sci. USA **100:**8957–8962.
4. **Bendtsen, J. D., H. Nielsen, G. von Heijne, and S. Brunak.** 2004. Improved prediction of signal peptides: SignalP 3.0. J. Mol. Biol. **340:**783–795.
5. **Bloom, M., G. A. Freyer, and D. A. Micklos.** 1995. Laboratory DNA science. Benjamin/Cummings Publishing Co., Inc., Redwood City, Calif.
6. **Buddington, K. K., J. B. Donahoo, and R. K. Buddington.** 2002. Dietary oligofructose and inulin protect mice from enteric and systemic pathogens and tumor inducers. J. Nutr. **132:**472–477.
7. **Burne, R. A., K. Schilling, W. H. Bowen, and R. E. Yasbin.** 1987. Expression, purification, and characterization of an exo-β-D-fructosidase of *Streptococcus mutans*. J. Bacteriol. **169:**4507–4517.
8. **Claesson, M. J., Y. Li, S. Leahy, C. Canchaya, J. P. van Pijkeren, A. M. Cerdeno-Tarraga, J. Parkhill, S. Flynn, G. C. O'Sullivan, J. K. Collins, D. Higgins, F. Shanahan, G. F. Fitzgerald, D. van Sinderen, and P. W. O'Toole.** 2006. Multireplicon genome architecture of *Lactobacillus salivarius*. Proc. Natl. Acad. Sci. USA **103:**6718–6723.
9. **Débarbouillé, M., I. Martin-Verstraete, F. Kunst, and G. Rapoport.** 1991. The *Bacillus subtilis sigL* gene encodes an equivalent of σ^{54} from gram-negative bacteria. Proc. Natl. Acad. Sci. USA **88:**9092–9096.
10. **Ehrmann, M. A., M. Korakli, and R. F. Vogel.** 2003. Identification of the gene for β-fructofuranosidase of *Bifidobacterium lactis* DSM10140^T and characterization of the enzyme expressed in *Escherichia coli*. Curr. Microbiol. **46:**391–397.
11. **Gibson, G. R., E. R. Beatty, X. Wang, and J. H. Cummings.** 1995. Selective stimulation of bifidobacteria in the human colon by oligofructose and inulin. Gastroenterology **108:**975–982.
12. **Gibson, G. R., and M. B. Roberfroid.** 1995. Dietary modulation of the human colonic microbiota: introducing the concept of prebiotics. J. Nutr. **125:**1401–1412.
13. **Gibson, G. R., and X. Wang.** 1994. Enrichment of bifidobacteria from human gut contents by oligofructose using continuous culture. FEMS Microbiol. Lett. **118:**121–127.
14. **Gionchetti, P., F. Rizzello, U. Helwig, A. Venturi, K. M. Lammers, P. Brigidi, B. Vitali, G. Poggioli, M. Miglioli, and M. Campieri.** 2003. Prophylaxis of pouchitis onset with probiotic therapy: a double-blind, placebo-controlled trial. Gastroenterology **124:**1202–1209.
15. **Hanahan, D.** 1985. Techniques for transformation of *E. coli*, p. 109–135. *In* D. M. Glover (ed.), DNA cloning: a practical approach, vol. 1. IRL Press Ltd., Oxford, England.
16. **Hidaka, H., T. Eida, T. Takizawa, T. Tokunaga, and Y. Tashiro.** 1986. Effects of fructooligosaccharides on intestinal flora and human health. Bifidobacteria Microflora **5:**37–50.
17. **Hidaka, H., M. Mirayama, and N. Sumi.** 1988. A fructooligosaccharide-producing enzyme from *Aspergillus niger* ATCC 20611. Agric. Biol. Chem. **52:**1181–1187.
18. **Hirayama, M., N. Sumi, and H. Hidaka.** 1989. Purification and properties of a fructooligosaccharide-producing β-fructofuranosidase from *Aspergillus niger* ATCC 20611. Agric. Biol. Chem. **53:**667–673.
19. **Imamura, L., K. Hisamitsu, and K. Kobashi.** 1994. Purification and characterization of β-fructofuranosidase from *Bifidobacterium infantis*. Biol. Pharm. Bull. **17:**596–602.
20. **Janer, C., L. M. Rohr, C. Pelaez, M. Laloi, V. Cleusix, T. Requena, and L. Meile.** 2004. Hydrolysis of oligofructose by the recombinant β-fructofuranosidase from *Bifidobacterium lactis*. Syst. Appl. Microbiol. **27:**279–285.
21. **Kajander, K., K. Hatakka, T. Poussa, M. Farkkila, and R. Korpela.** 2005. A probiotic mixture alleviates symptoms in irritable bowel syndrome patients: a controlled 6-month intervention. Aliment. Pharmacol. Ther. **22:**387–394.
22. **Kaplan, H., and R. W. Hutkins.** 2003. Metabolism of fructooligosaccharides by *Lactobacillus paracasei* 1195. Appl. Environ. Microbiol. **69:**2217–2222.
23. **Kleerebezem, M., J. Boekhorst, R. van Kranenburg, D. Molenaar, O. P. Kuipers, R. Leer, R. Tarchini, S. A. Peters, H. M. Sandbrink, M. W. E. J. Fiers, W. Stiekema, R. M. K. Lankhorst, P. A. Bron, S. M. Hoffer, M. N. N. Groot, R. Kerkhoven, M. de Vries, B. Ursing, W. M. de Vos, and R. J. Siezen.** 2003. Complete genome sequence of *Lactobacillus plantarum* WCFS1. Proc. Natl. Acad. Sci. USA **100:**1990–1995.
24. **Law, J., G. Buist, A. Haandrikman, J. Kok, G. Venema, and K. Leenhouts.** 1995. A system to generate chromosomal mutations in *Lactococcus lactis* which allows fast analysis of targeted genes. J. Bacteriol. **177:**7011–7018.
25. **Leenhouts, K., G. Buist, A. Bolhuis, A. ten Berge, J. Kiel, I. Mierau, M. Dabrowska, G. Venema, and J. Kok.** 1996. A general system for generating unlabelled gene replacements in bacterial chromosomes. Mol. Gen. Genet. **253:**217–224.
26. **Maguin, E., P. Duwat, T. Hege, D. Ehrlich, and A. Gruss.** 1992. New thermosensitive plasmid for gram-positive bacteria. J. Bacteriol. **174:**5633–5638.
27. **Makras, L., G. Van Acker, and L. De Vuyst.** 2005. *Lactobacillus paracasei* subsp. *paracasei* 8700:2 degrades inulin-type fructans exhibiting different degrees of polymerization. Appl. Environ. Microbiol. **71:**6531–6537.
28. **Mazé, A., G. Boël, S. Poncet, I. Mijakovic, Y. Le Breton, A. Benachour, V. Monedero, J. Deutscher, and A. Hartke.** 2004. The *Lactobacillus casei ptsH*147T mutation causes overexpression of a LevR-regulated but RpoN-independent operon encoding a mannose class phosphotransferase system. J. Bacteriol. **186:**4543–4555.
29. **Miwa, Y., A. Nakata, A. Ogiwara, M. Yamamoto, and Y. Fujita.** 2000. Evaluation and characterization of catabolite-responsive elements (*cre*) of *Bacillus subtilis*. Nucleic Acids Res. **28:**1206–1210.
30. **Muller, M., and W. Seyfarth.** 1997. Purification and substrate specificity of an extracellular fructanhydrolase from *Lactobacillus paracasei* ssp. *paracasei* P4134. New Phytol. **136:**89–96.
31. **Muramatsu, K., S. Onodera, M. Kikuchi, and N. Shiomi.** 1992. The production of β-fructofuranosidase from *Bifidobacterium* spp. Biosci. Biotechnol. Biochem. **56:**1451–1454.

32. **Muramatsu, K., S. Onodera, M. Kikuchi, and N. Shiomi.** 1993. Purification and some properties of β-fructofuranosidase from *Bifidobacterium adolescentis* G1. Biosci. Biotechnol. Biochem. **57:**1681–1685.
33. **Muramatsu, K., S. Onodera, M. Kikuchi, and N. Shiomi.** 1994. Substrate specificity and subsite affinities of β-fructofuranosidase from *Bifidobacterium adolescentis* G1. Biosci. Biotechnol. Biochem. **58:**1642–1645.
34. **Naumov, D. G., and V. G. Doroshenko.** 1998. β-Fructosidases: a new superfamily of glycosyl hydrolases. Mol. Biol. **32:**761–766.
35. **Navarre, W. W., and O. Schneewind.** 1999. Surface proteins of gram-positive bacteria and mechanisms of their targeting to the cell wall envelope. Microbiol. Mol. Biol. Rev. **63:**174–229.
36. **Nemcová, R., A. Bomba, S. Gancarcikova, R. Herich, and P. Guba.** 1999. Study of the effect of *Lactobacillus paracasei* and fructooligosaccharides on the faecal microflora in weanling piglets. Berl. Munch. Tierarztl. Wochenschr. **112:**225–228.
37. **Niness, K. R.** 1999. Inulin and oligofructose: what are they? J. Nutr. **129:** 1402S–1406S.
38. **Oku, T., T. Tokunaga, and N. Hosoya.** 1984. Nondigestibility of a new sweetener, Neosugar, in the rat. J. Nutr. **114:**1574–1581.
39. **Paludan-Müller, C., L. Gram, and F. P. Rattray.** 2002. Purification and characterisation of an extracellular fructan β-fructosidase from a *Lactobacillus pentosus* strain isolated from fermented fish. Syst. Appl. Microbiol. **25:**13–20.
40. **Perrin, S., M. Warchol, J. P. Grill, and F. Schneider.** 2001. Fermentations of fructo-oligosaccharides and their components by *Bifidobacterium infantis* ATCC 15697 on batch culture in semi-synthetic medium. J. Appl. Microbiol. **90:**859–865.
41. **Pons, T., O. Olmea, G. Chinea, A. Beldarrain, G. Marquez, N. Acosta, L. Rodriguez, and A. Valencia.** 1998. Structural model for family 32 of glycosylhydrolase enzymes. Proteins **33:**383–395.
42. **Pridmore, R. D., B. Berger, F. Desiere, D. Vilanova, C. Barretto, A.-C. Pittet, M.-C. Zwahlen, M. Rouvet, E. Altermann, R. Barrangou, B. Mollet, A. Mercenier, T. Klaenhammer, F. Arigoni, and M. A. Schell.** 2004. The genome sequence of the probiotic intestinal bacterium *Lactobacillus johnsonii* NCC 533. Proc. Natl. Acad. Sci. USA **101:**2512–2517.
43. **Rosenow, C., M. Maniar, and J. Trias.** 1999. Regulation of the α-galactosidase activity in *Streptococcus pneumoniae*: characterization of the raffinose utilization system. Genome Res. **9:**1189–1197.
44. **Rudi, K., T. Fossheim, and K. S. Jakobsen.** 1999. Restriction cutting independent method for cloning genomic DNA segments outside the boundaries of known sequences. BioTechniques **27:**1170–1177.
45. **Russell, R. R. B., J. Aduse-Opoku, I. C. Sutcliffe, L. Tao, and J. J. Ferretti.** 1992. A binding protein-dependent transport system in *Streptococcus mutans* responsible for multiple sugar metabolism. J. Biol. Chem. **267:**4631–4637.
46. **Russell, W. M., and T. R. Klaenhammer.** 2001. Efficient system for directed integration into the *Lactobacillus acidophilus* and *Lactobacillus gasseri* chromosome via homologous recombination. Appl. Environ. Microbiol. **67:** 4361–4364.
47. **Saggioro, A.** 2004. Probiotics in the treatment of irritable bowel syndrome. J. Clin. Gastroenterol. **38:**S104–S106.
48. **Schell, M. A., M. Karmirantzou, B. Snel, D. Vilanova, B. Berger, G. Pessi, M.-C. Zwahlen, F. Desiere, P. Bork, M. Delley, R. D. Pridmore, and F. Arigoni.** 2002. The genome sequence of *Bifidobacterium longum* reflects its adaptation to the human gastrointestinal tract. Proc. Natl. Acad. Sci. USA **99:**14422–14427.
49. **van de Guchte, M., S. Penaud, C. Grimaldi, V. Barbe, K. Bryson, P. Nicolas, C. Robert, S. Oztas, S. Mangenot, A. Couloux, V. Loux, R. Dervyn, R. Bossy, A. Bolotin, J. M. Batto, T. Walunas, J. F. Gibrat, P. Bessieres, J. Weissenbach, S. D. Ehrlich, and E. Maguin.** 2006. The complete genome sequence of *Lactobacillus bulgaricus* reveals extensive and ongoing reductive evolution. Proc. Natl. Acad. Sci. USA **103:**9274–9279.
50. **Warchol, M., S. Perrin, J.-P. Grill, and F. Schneider.** 2002. Characterization of a purified β-fructosidase from *Bifidobacterium infantis* ATCC 15697. Lett. Appl. Microbiol. **35:**462–467.
51. **Wei, M.-Q., C. M. Rush, J. M. Norman, L. M. Hafner, R. J. Epping, and P. Timms.** 1995. An improved method for the transformation of *Lactobacillus* strains using electroporation. J. Microbiol. Methods **21:**97–109.
52. **Williams, C. H., S. A. Witherly, and R. K. Buddington.** 1994. Influence of dietary Neosugar on selected bacterial groups of the human faecal microbiota. Microb. Ecol. Health Dis. **7:**91–97.

Supplemental Figure 1. Sequence alignment of the *L. paracasei* 1195 β-fructosidase (FosE), *L. casei* fructan hydrolase (LevH1; BAD88632), and *L. casei* ATCC 334 β-fructosidase (Bfr; ZP_00386222). Conserved motifs of the GH family 32 are highlighted. The conserved Asp (♦) and Cys (◊) residues potentially involved in either catalytic or substrate-binding activity are indicated. Vertical arrow specifies the potential cleavage site of signal peptidase. Cell wall anchor motifs (LPX[T/A]G) for all three enzymes are double-lined. The start locations of each 80-amino acid repeat of FosE are indicated with horizontal arrows; sequences of the 53-amino acid-repeat (pfam06458) are underlined. A segment of 80 amino acids in length that is present in FosE but not in LevH1 is indicated in bold type face. Only the first 806 residues of BfrA showed significant homology to FosE and LevH1, and the 80-residue repeat sequences were not found in this enzyme. Rather, BfrA contains two copies of 53-amino acid repeats that are specific for peptidoglycan bound proteins. These repeats correspond to residue 762 to 814 and 832 to 884 of the enzyme precursor. Partial sequence of the repeat (37/53 residues) was also observed in FosE (residue 750 to 786) and LexH1 (residue 748 to 784).

Supplemental Figure 1, Goh *et al.*

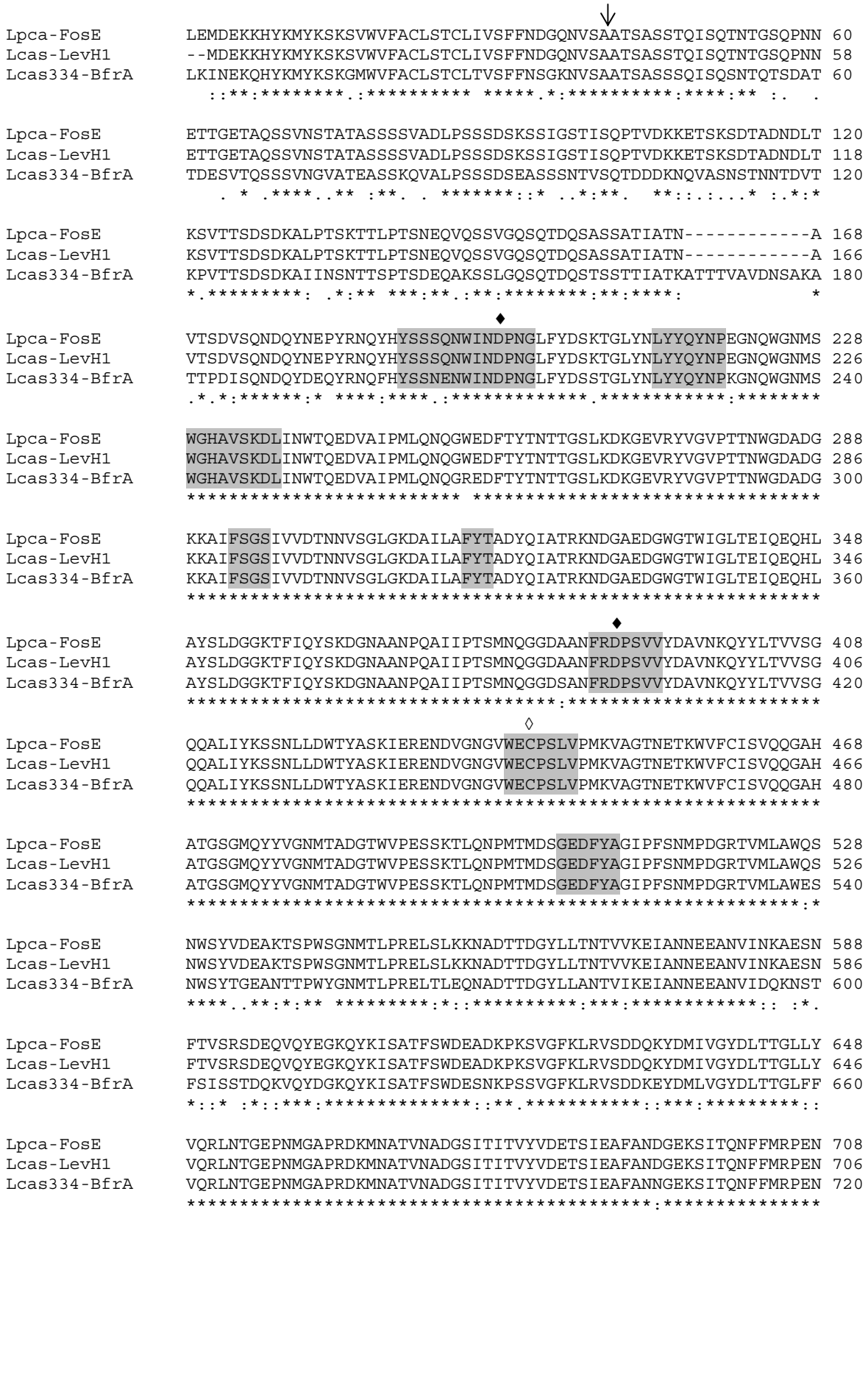

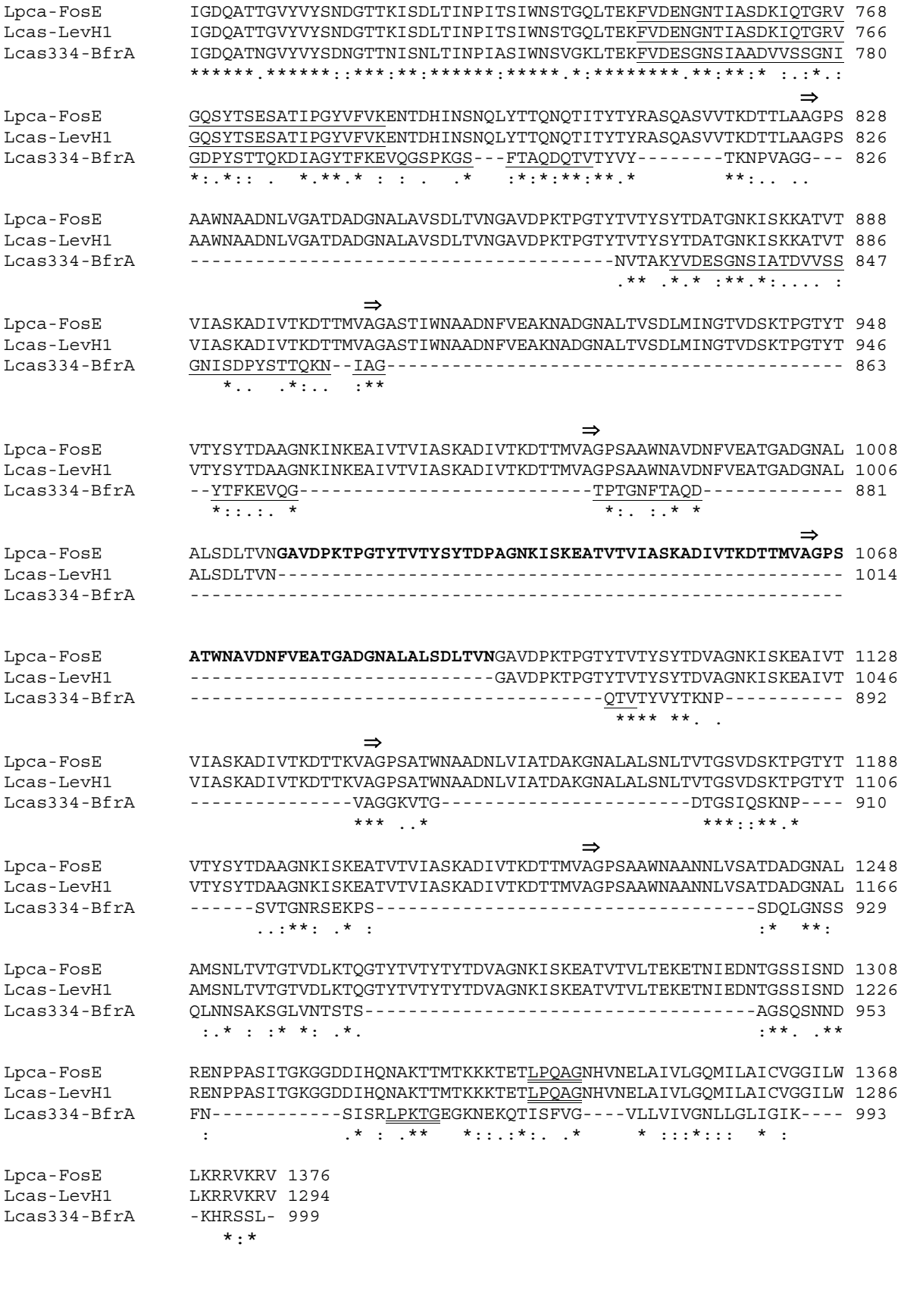
Lpca-FosE IGDQATTGVYVYSNDGTTKISDLTINPITSIWNSTGQLTEKFVDENGNTIASDKIQTGRV 768
Lcas-LevH1 IGDQATTGVYVYSNDGTTKISDLTINPITSIWNSTGQLTEKFVDENGNTIASDKIQTGRV 766
Lcas334-BfrA IGDQATNGVYVYSDNGTTNISNLTINPIASIWNSVGKLTEKFVDESGNSIAADVVSSGNI 780
Lpca-FosE GQSYTSESATIPGYVFVKENTDHINSNQLYTTQNQTITYTYRASQASVVTKDTTLAAGPS 828
Lcas-LevH1 GQSYTSESATIPGYVFVKENTDHINSNQLYTTQNQTITYTYRASQASVVTKDTTLAAGPS 826
Lcas334-BfrA GDPYSTTQKDIAGYTFKEVQGSPKGS---FTAQDQTVTYVY--------TKNPVAGG--- 826
Lpca-FosE AAWNAADNLVGATDADGNALAVSDLTVNGAVDPKTPGTYTVTYSYTDATGNKISKKATVT 888
Lcas-LevH1 AAWNAADNLVGATDADGNALAVSDLTVNGAVDPKTPGTYTVTYSYTDATGNKISKKATVT 886
Lcas334-BfrA ----------NVTAKYVDESGNSIATDVVSS 847
Lpca-FosE VIASKADIVTKDTTMVAGASTIWNAADNFVEAKNADGNALTVSDLMINGTVDSKTPGTYT 948
Lcas-LevH1 VIASKADIVTKDTTMVAGASTIWNAADNFVEAKNADGNALTVSDLMINGTVDSKTPGTYT 946
Lcas334-BfrA GNISDPYSTTQKN--IAG---------- 863
Lpca-FosE VTYSYTDAAGNKINKEAIVTVIASKADIVTKDTTMVAGPSAAWNAVDNFVEATGADGNAL 1008
Lcas-LevH1 VTYSYTDAAGNKINKEAIVTVIASKADIVTKDTTMVAGPSAAWNAVDNFVEATGADGNAL 1006
Lcas334-BfrA --YTFKEVQG----------TPTGNFTAQD---------- 881
Lpca-FosE ALSDLTVNGAVDPKTPGTYTVTYSYTDPAGNKISKEATVTVIASKADIVTKDTTMVAGPS 1068
Lcas-LevH1 ALSDLTVN---------- 1014
Lcas334-BfrA ----------
Lpca-FosE ATWNAVDNFVEATGADGNALALSDLTVNGAVDPKTPGTYTVTYSYTDVAGNKISKEAIVT 1128
Lcas-LevH1 ----------GAVDPKTPGTYTVTYSYTDVAGNKISKEAIVT 1046
Lcas334-BfrA ----------QTVTYVYTKNP---------- 892
Lpca-FosE VIASKADIVTKDTTKVAGPSATWNAADNLVIATDAKGNALALSNLTVTGSVDSKTPGTYT 1188
Lcas-LevH1 VIASKADIVTKDTTKVAGPSATWNAADNLVIATDAKGNALALSNLTVTGSVDSKTPGTYT 1106
Lcas334-BfrA ----------VAGGKVTG----------DTGSIQSKNP---- 910
Lpca-FosE VTYSYTDAAGNKISKEATVTVIASKADIVTKDTTMVAGPSAAWNAANNLVSATDADGNAL 1248
Lcas-LevH1 VTYSYTDAAGNKISKEATVTVIASKADIVTKDTTMVAGPSAAWNAANNLVSATDADGNAL 1166
Lcas334-BfrA ------SVTGNRSEKPS----------SDQLGNSS 929
Lpca-FosE AMSNLTVTGTVDLKTQGTYTVTYTYTDVAGNKISKEATVTVLTEKETNIEDNTGSSISND 1308
Lcas-LevH1 AMSNLTVTGTVDLKTQGTYTVTYTYTDVAGNKISKEATVTVLTEKETNIEDNTGSSISND 1226
Lcas334-BfrA QLNNSAKSGLVNTSTS----------AGSQSNND 953
Lpca-FosE RENPPASITGKGGDDIHQNAKTTMTKKKTETLPQAGNHVNELAIVLGQMILAICVGGILW 1368
Lcas-LevH1 RENPPASITGKGGDDIHQNAKTTMTKKKTETLPQAGNHVNELAIVLGQMILAICVGGILW 1286
Lcas334-BfrA FN----------SISRLPKTGEGKNEKQTISFVG----VLLVIVGNLLGLIGIK---- 993
Lpca-FosE LKRRVKRV 1376
Lcas-LevH1 LKRRVKRV 1294
Lcas334-BfrA -KHRSSL- 999